HHS Public Access

Author manuscript

IEEE Trans Neural Syst Rehabil Eng. Author manuscript; available in PMC 2020 October 21.

Published in final edited form as:

IEEE Trans Neural Syst Rehabil Eng. 2019 July ; 27(7): 1467–1472. doi:10.1109/TNSRE.2019.2912298.

Hemicraniectomy in traumatic brain injury: a noninvasive platform to investigate high gamma activity for brain machine interfaces

Mukta Vaidya,
Department of Neurology, Northwestern University, Chicago, IL 60611 USA

Robert D. Flint,
Department of Neurology, Northwestern University, Chicago, IL 60611 USA

Po T. Wang,
Department of Biomedical Engineering, University of California-Irvine, CA 92697 USA

Alex Barry,
Shirley Ryan Ability Lab, Chicago, IL 60611 USA

Yongcheng Li,
Department of Neurology, University of California-Irvine, CA 92697 USA

Mohammad Ghassemi,
Department of Biomedical Engineering, North Carolina State University, Raleigh, NC 27695 USA

Goran Tomic,
Department of Neurology, Northwestern University, Chicago, IL 60611 USA

Jun Yao,
Physical Therapy & Human Movement Science, Northwestern University, Chicago, IL 60611 USA

Carolina Carmona,
Physical Therapy & Human Movement Science, Northwestern University, Chicago, IL 60611 USA

Emily M. Mugler,
Department of Neurology, Northwestern University, Chicago, IL 60611 USA

Sarah Gallick,
Shirley Ryan Ability Lab, Chicago, IL 60611 USA

Sangeeta Driver,
Shirley Ryan Ability Lab and the Department of Physician Medicine & Rehabilitation, Northwestern University, Chicago, IL 60611 USA

Nenad Brkic,
Shirley Ryan Ability Lab and the Department of Physician Medicine & Rehabilitation, Northwestern University, Chicago, IL 60611 USA

David Ripley,

mukta.vaidya@northwestern.edu.

Shirley Ryan Ability Lab and the Department of Physician Medicine & Rehabilitation, Northwestern University, Chicago, IL 60611 USA

Charles Liu,
Rancho Los Amigos National Center for Rehabilitation and the Department of Neurosurgery, University of Southern California, Los Angeles, CA 90007 USA

Derek Kamper,
Department of Biomedical Engineering, North Carolina State University, Raleigh, NC 27695 USA

An H. Do,
Rancho Los Amigos National Center for Rehabilitation and the Department of Neurology, University of California-Irvine, CA 92697 USA

Marc W. Slutzky [Senior Member, IEEE]
Departments of Neurology, Physiology, and Physical Medicine & Rehabilitation, Northwestern University and the Shirley Ryan Ability Lab, Chicago, IL 60611 USA

Abstract

Brain-machine interfaces (BMIs) translate brain signals into control signals for an external device, such as a computer cursor or robotic limb. These signals can be obtained either noninvasively or invasively. Invasive recordings, using electrocorticography (ECoG) or intracortical microelectrodes, provide higher bandwidth, more informative signals. Rehabilitative BMIs, which aim to drive plasticity in the brain to enhance recovery after brain injury, have almost exclusively used non-invasive recordings, such electroencephalography (EEG) or magnetoencephalography (MEG), which have limited bandwidth and information content. Invasive recordings provide more information and spatiotemporal resolution, but do incur risk, and thus are not usually investigated in people with stroke or traumatic brain injury (TBI). Here, we describe a new BMI paradigm to investigate the use of higher frequency signals in brain-injured subjects without incurring significant risk. We recorded EEG in TBI subjects who required hemicraniectomies (removal of part of the skull). EEG over the hemicraniectomy (hEEG) contained substantial information in the high gamma frequency range (65-115 Hz). Using this information, we decoded continuous finger flexion force with moderate to high accuracy (variance accounted for 0.06 to 0.52), which at best approaches that using epidural signals. These results indicate that people with hemicraniectomies can provide a useful resource for developing BMI therapies for the treatment of brain injury.

Keywords

brain machine interface; brain computer interface; EEG; traumatic brain injury; high gamma

I. INTRODUCTION

BRAIN-MACHINE interfaces (BMIs) translate brain signals, obtained via both non-invasive and invasive methods, into control signals for some external device, such as a computer cursor or robotic limb. BMIs that seek to replace function through the control of an external device are termed assistive BMIs. Recently, groups have begun to investigate BMIs for rehabilitation, aiming to enhance the brain's own recovery after stroke or injury instead of

replacing function [1], [2]. The concept of rehabilitative BMIs is to drive plasticity, most likely by facilitating some type of simultaneous pre- and post-synaptic activity [3]. Yet, these types of BMIs have almost exclusively relied on non-invasive methods, such as EEG or MEG, which provide limited bandwidth (<30 Hz for EEG) and spatiotemporal resolution.

Signals obtained with invasive recording techniques, such as subdural ECoG or intracortical microelectrodes, provide higher bandwidth, and more informative, signals, such as neural spiking activity or broadband high gamma activity (HG, 65–115Hz) for BMI control [4]–[6]. The higher spatiotemporal resolution and information content of neural signals obtained invasively, such as high gamma [7], may enable BMIs to drive plasticity more effectively due to enhanced synchrony between co-activated regions. However, the risks and expenses associated with the surgery required to implant intracranial electrodes form a formidable barrier to investigating BMIs that use higher fidelity invasive signals in potential end-users. Here, we propose a new paradigm to address such limitations: BMIs that use the HG acquired from the scalp in people with traumatic brain injuries.

Some patients with severe traumatic brain injury (TBI) require hemicraniectomies—removal of part of the skull to alleviate or control intracranial pressure—to prevent brain herniation [8]. The patients often wait multiple weeks to several months until the piece of skull is replaced [9]. Without the highly-dense skull present, the EEG over the hemicraniectomy (hEEG) provides signals with higher amplitude [10], as well as higher spatial resolution [11].

hEEG signals from motor areas have increased amplitude and bandwidth, including HG band, and have been shown to modulate with hand movement onset, albeit in a limited sample [12]. Analogous studies, using invasive techniques, have shown finger kinematics during grasp movements can be decoded accurately using high gamma signals from subdural [13], [14] and epidural [14] electrodes. Finger pinch force can also be decoded with high accuracy using the HG from ECoG [15].

Here, we investigated the suitability of the hemicraniectomy model in TBI survivors as an approach for developing rehabilitative BMIs for the treatment of people with brain injuries. We designed an automated method to reduce muscle and eye artifact-related information, while preserving relevant high-gamma information, from the hEEG signals of these subjects. We examined the extent to which HG in hEEG can be used to decode continuous pinch force. We worked with TBI survivors that had received hemicraniectomies and were undergoing acute inpatient rehabilitation. We found that hEEG carried sufficient information in the high gamma range to decode finger flexion force with reasonably good accuracy. The ability to decode grasp force is particularly important in BMIs that are intended to restore grasp (via FES or prosthetic hands). These results indicate that this paradigm is a useful platform for developing both rehabilitative and assistive brain-machine interfaces for the treatment of traumatic brain injury, and possibly for stroke as well.

II. METHODS

A. Neural Recordings

We recorded from seven adult participants who had undergone decompressive hemicraniectomies after suffering traumatic brain injuries. All participants in the study signed informed consent forms. Experiments were conducted in Chicago, at the Rehabilitation Institute of Chicago (subjects A, B, & C) and the Shirley Ryan Ability Lab–the new name for the Rehabilitation Institute of Chicago, subjects D & G–and at the Rancho Los Amigos National Center for Rehabilitation in Los Angeles (subjects E & F). Experimental protocols were approved by the Institutional Review Boards of Northwestern University and Rancho Los Amigos National Rehabilitation Center. Subjects A, E, and F underwent hemicraniectomies over their left hemisphere, while subjects B, C, D, and G underwent hemicraniectomies over their right hemisphere. For subjects D, E, F, & G (18 of the 23 datasets), the location of the hemicraniectomy was demarcated with respect to the EEG electrodes, whereas, in the case of subjects A, B, & C (5 of the 23 datasets), only the hemisphere of the hemicraniectomy was recorded. All sessions were conducted prior to cranioplasty. For subject A, EEG was recorded using a 64-electrode actiCAP (Brain Products, Inc.). For subject B, EEG was recorded using a 160-electrode headcap with the Active2 system (Biosemi, Inc.). In all other subjects, EEG was recorded using a 128-electrode actiCAP (Figure 1A, 1B). To ensure good contact between electrodes and the skin over the craniectomy, we placed several sheets of cotton gauze on top of the cap over the craniectomy side, then wrapped the cap gently with kerlix gauze. EEG signals from all cap types were amplified, filtered with a pass-band from 0.3 to 500 Hz, and sampled at 2 kHz using a Neuroport Acquisition System (Blackrock Microsystems).

B. Behavioral Task

Subjects performed a 1-dimensional continuous force-matching task (Figure 1C) with their arms resting in their lap while sitting in a chair or in their hospital bed. Subjects pressed on a load cell by flexing the thumb contralateral to their hemicraniectomy site. The generated force controlled the one-dimensional position of a cursor on a screen placed in front of the subject. Targets appeared at randomly selected force levels ranging from 0 to 70 N. The subject had three seconds to hit a target by generating the appropriate force on the load cell with their thumb and holding within the target for 100 ms. At the end of each trial, the target would disappear, and a new target would appear one second later. A daily session consisted of one or more runs: each run lasted 5 minutes, ranging from 15–51 trials. A total of 23 runs across the 7 subjects were analyzed for this study.

C. Artifact Removal

Since EEG can be contaminated by artifacts from eye movements (EOG) and head and neck muscles (EMGs), we sought to remove these artifacts from hEEG. We modified established methods, which are focused largely on low-frequency, EOG artifacts. Using EEGLAB [16], we first low-pass filtered the data at 300 Hz with a two-way least squares FIR filter, and then performed independent component analysis (ICA) on the data. We created a novel, automated method, termed annular component removal (ACR), for artifact removal using these components. More specifically, in ACR, the components were first categorized into

two regions of activation. The central region was composed of electrodes that were posterior to and including the F-row, anterior to and including the P-row, and no more lateral than column 5/6 (Figure 1D). The peripheral region was composed of all other electrodes, including those anterior to the F-row, posterior to the P-row, or more lateral than column 5/6. Components that had activation levels on the periphery equal to or larger than activation in the central region were marked as being dominated by EMG or EOG artifact, since both of these artifacts originate from peripheral sources [17]. We subtracted the projections from these components from the EEG prior to further analysis to remove such artifacts. Since broadband (0–300 Hz) EEG, and thus components derived from it using ICA, are dominated by low frequencies, we employed an extra step to ensure we also removed artifacts specific to the high-gamma frequency range (which is particularly important to remove broadband EMG). In addition, we re-processed the data using the same methods as stated above, but with a band-pass filter of 65–115 Hz (HG) instead of a low-pass filter of 300Hz. Our artifact removal method generated two types of data in the time domain: the high-gamma artifact-removed data and the broadband artifact-removed data were used for the remainder of the analysis.

D. Feature Extraction

We used time-varying power as EEG features. To create EEG features, we common average referenced the high-gamma artifact-removed data. We computed FFTs in a series of shifted time windows (window size: 256 ms, window overlap: 206 ms) and squared the resulting amplitudes to compute time-varying power. In addition, we used the same method with the broadband artifact-removed data to compute the power in four frequency bands for each electrode—delta (<4 Hz), mu (7 to 12 Hz), beta (12 to 30 Hz), and HG—in addition to computing the local motor potential (LMP, mean amplitude in the same window [18],[15], [19]). The power in each 50-ms bin was log-normalized—the log of the mean power over the entire run for each electrode was subtracted off from the log of the time-varying power of that electrode [14].

E. Correlation High Gamma with Force

To examine the relationship between force and high gamma on individual electrodes, we subsampled the force from 2 kHz to 20 Hz and smoothed both the force and high gamma power using a moving average filter of 1 second width, with filter coefficients equal to the reciprocal of the span. Pearson’s correlation coefficients were calculated between the force and time-varying log HG power for each electrode. Differences between distributions of correlation coefficients were tested for significance using single-tailed t-tests.

F. Decoding Force

For decoding force, the raw force signal was first smoothed using a moving average filter with a width of 256 ms and interpolated down to a resolution of 20 Hz to match the resolution of the EEG features. For subjects D, E, and F, we restricted the electrodes used for decoding to those directly above the hemicraniectomy that were also in the central region (see Methods: Artifact Removal). In the case of subjects A, B, and C, since only hemispheric information on the craniectomy was available, we restricted the electrodes used for decoding to those in the recorded craniectomy hemisphere (not including the z-electrodes) that were

also in the central region. For each run, we compared the decoding performance using only HG power vs. using all the lower power bands plus LMP. Decoders were built using techniques similar to those we have used in the past [15], [19]. Using training data, we first ranked the features by the absolute value of their correlation coefficients with force and selected the top 50% of these features. We built Wiener cascade filters [20], [21] with 3rd-order polynomial nonlinearities with 10 taps (10 bins of 50 ms each), using ridge regression to reduce potential overfitting [22]. Decoder input features were derived from all of the electrodes above the hemicraniectomy (hEEG), and from all the homologous electrodes, of the same mediolateral and anteroposterior locations, on the contralateral hemisphere (cEEG). For example, if C3 was over the hemicraniectomy, the homologous contralateral electrode would be C4. We used 10-fold cross-validation to generate the mean performance (measured as the variance in actual force accounted for by decoded force) in each run. The variance accounted for (VAF) was computed as $VAF = 1 - \frac{SSres}{SStot}$, where $SSres$ was the residual sum of squares and $SStot$ was the total sum of squares. Differences in decoding performance were tested for significance using single-tailed, paired t-tests.

III. RESULTS

We recorded from seven adult subjects with varying degrees of weakness in their hands, with Action Research Arm Test (ARAT) scores ranging from 39/57 to 57/57. We found substantial high-gamma activity using hEEG in all seven subjects. HG activity from hEEG electrodes (Figure 2A) were more highly correlated with force (mean ± SD R=0.13 ± 0.22) than those from cEEG electrodes (R=0.05 ± 0.20) after ACR (Figures 2B, 2C; $p=4\times10^{-7}$). ACR preserved the movement-related information in hEEG HG (Figure 2D, no difference in correlation distributions; p = 0.6).

We decoded force with moderate to high accuracy (mean ± SEM VAF of 0.21 ± 0.02 over all subjects, range of 0.06 to 0.52) using just the high gamma signals from hEEG after ACR (Figure 3).

The decoding performance using HG alone was highly correlated (Figure 4A, R=0.51, p=0.01) with that using all frequency bands plus the LMP (all-bands VAF = 0.27 ± 0.03). Moreover, decoding performance was higher using HG from hEEG than from the cEEG (Figure 4B, cEEG VAF of 0.19 ± 0.02; p=0.008). This suggests that HG from hEEG contains cortically sourced force-related information above and beyond potential artifact which could be present in the HG range. Decoding performance was marginally better in subjects for whom we marked the exact location of the hemicraniectomy relative to the electrodes than in subjects with unmarked hemicraniectomies (VAF = 0.23 ± 0.03 vs. 0.15 ± 0.03 for marked and unmarked, respectively; p = 0.09). ACR preserved the hEEG HG-only decoding performance (no significant performance difference before and after artifact removal, Figure 4C, p = 0.40), while only marginally preserving cEEG HGonly decoding performance (Figure 4D, p = 0.07), and not preserving the hEEG all-feature performance (p = 0.01).

IV. DISCUSSION

These results demonstrate the ability to obtain high gamma band activity using hEEG in people with TBI. The high gamma activity contained substantial information about finger flexion force, enough to decode continuous force with reasonably high accuracy. The best performances approached levels observed in similar epidural and ECoG studies of finger force and movement decoding [14], [15]. Further, decoding accuracy using HG was comparable to that using all frequency bands and the LMP (see Figure 4A), which implies that hEEG provides highly informative, high-bandwidth signals.

Prior studies have shown that grasping kinematics can be decoded accurately using HG information in subdural [13], [14], [23], [24] and epidural [14] signals (VAF 0.4±0.04). HG information in ECoG can also decode finger precision pinch force with high accuracy [15]. The decoding performances observed in these studies ranged from comparable to substantially better than the distribution of decoding performances we observed using hEEG. This is not surprising, given that ECoG is much closer to the cortical source, while hEEG still has attenuation from the CSF and skin [11]. ECoG is also much less susceptible to EMG and EOG artifacts [25]. Indeed, it is encouraging that the best several hEEG channels performed nearly as well as epidural signals, especially in epidural recordings using more coarsely-spaced electrodes (1 cm, which is closer to the hEEG spacing here) [14]. These results indicate that the TBI hemicraniectomy paradigm may be a useful platform for developing BMI therapies for brain-injured patients.

We developed an automated method, ACR, to reduce muscle and eye artifact-related information in the signals recorded from these patients. After artifact removal, there was still was some information in the high gamma range in cEEG (Figure 4B). One potential explanation is that the high-gamma band activity recorded on the non-craniectomy hemisphere were derived from ipsilateral cortical activation with motor activity, which has been reported using invasive recordings during reaching [26], and that it could be recorded through the skull, which has also been reported [27], [28]. Another explanation could be that there was insufficient EMG artifact removal [29]. We have found that there is inherent tradeoff between removing muscle-related artifact and retaining relevant HG signal from cortical sources. Notably, the difference in the means of the distributions of force-hEEG and force-cEEG correlation coefficients was significant, but small ($R = 0.08$), Given that high gamma activity is highly localized in the brain, we would not necessarily expect the majority of hEEG electrodes to have substantially greater force-related HG activation than the cEEG, but rather just a few hEEG electrodes in each dataset.

The greatest advantage to hEEG is that it enables viable non-invasive recording of high-bandwidth signals, allowing for the development of rehabilitative or assistive BMIs in a potential end-user population (TBI patients). To date, several assistive BMI studies using high-bandwidth signals from invasive recording techniques have been conducted in end-user populations [30]–[35]. Notably, these studies included only 1–3 subjects each. Only one studies has investigated the feasibility of a rehabilitative BMI using epidural signals; again in one person [36]. While two studies have shown that a modest amount of HG can be recorded from EEG [27], [28], neither single-trial nor continuous decoding was demonstrated. The

hEEG-based paradigm enables concurrent research and development of BMIs in TBI patients, providing the ability to test feasibility and design and to optimize both to benefit patients. This platform can also enable prototyping of invasive BMI paradigms (mainly epidural or subdural) without significant risk to patients, allowing for larger patient cohorts to be studied, which is important for testing clinical treatments. For example, we are examining the extent to which a hEEG-based BMI can help to rehabilitate motor function in TBI patients. If successful, this investigation could potentially lead to investigations of moderately invasive BMIs for the rehabilitation or replacement of function in patients with TBI, a leading causes of death and disability worldwide [37], and possibly for stroke as well.

ACKNOWLEDGEMENTS

In addition, the authors would like to thank Zachary Wright and Julius Dewald for their assistance in this study.

This work was supported by NIH grantR01NS094748, and Doris Duke Charitable Foundation Clinical Scientist Development Award (Grant #2011039).

REFERENCES

[1]. Ang KK. A clinical study of motor imagery-based brain-computer interface for upper limb robotic rehabilitation; 2009 Annual International Conference of the IEEE Engineering in Medicine and Biology Society; 2009. 5981–5984.

[2]. Ramos-Murguialday A. et al., “Brain-Machine-Interface in Chronic Stroke Rehabilitation: A Controlled Study,” Ann. Neurol, vol. 74, no. 1, pp. 100–108, 7 2013. [PubMed: 23494615]

[3]. Soekadar SR, Birbaumer N, Slutzky MW, and Cohen LG, “Brain–machine interfaces in neurorehabilitation of stroke,” Neurobiol. Dis, vol. 83, pp. 172–179, 11 2015. [PubMed: 25489973]

[4]. Slutzky MW and Flint RD, “Physiological properties of brain-machine interface input signals,” J. Neurophysiol, vol. 118, no. 2, pp. 1329–1343, 6 2017. [PubMed: 28615329]

[5]. Slutzky MW, “Brain-Machine Interfaces: Powerful Tools for Clinical Treatment and Neuroscientific Investigations,” The Neuroscientist, p. 1073858418775355, 5 2018.

[6]. Slutzky MW and Flint RD, “Physiological Properties of Brain Machine Interface Input Signals,” J. Neurophysiol, p. jn.00070.2017, 6 2017.

[7]. Crone NE, Boatman D, Gordon B, and Hao L, “Induced electrocorticographic gamma activity during auditory perception,” Clin. Neurophysiol, vol. 112, no. 4, pp. 565–582, 4 2001. [PubMed: 11275528]

[8]. Holland M. and Nakaji P, “Craniectomy: surgical indications and technique,” Oper. Tech. Neurosurg, vol. 7, no. 1, pp. 10–15, 3 2004.

[9]. Archavlis E. and Nievas MCY, “The impact of timing of cranioplasty in patients with large cranial defects after decompressive hemicraniectomy,” Acta Neurochir. (Wien), vol. 154, no. 6, pp. 1055–1062, 6 2012. [PubMed: 22527574]

[10]. Niedermeyer E, “The ‘Third Rhythm’: Further Observations,” Clin. Electroencephalogr, vol. 22, no. 2, pp. 83–96, 4 1991. [PubMed: 2032348]

[11]. Slutzky MW, Jordan LR, Krieg T, Chen M, Mogul DJ, and Miller LE, “Optimal spacing of surface electrode arrays for brain–machine interface applications,” J. Neural Eng, vol. 7, no. 2, p. 026004, 2010.

[12]. Voytek B. et al., “Hemicraniectomy: A New Model for Human Electrophysiology with High Spatio-temporal Resolution,” J. Cogn. Neurosci, vol. 22, no. 11, pp. 2491–2502, 11 2009.

[13]. Kubánek J, Miller KJ, Ojemann JG, Wolpaw JR, and Schalk G, “Decoding flexion of individual fingers using electrocorticographic signals in humans,” J. Neural Eng, vol. 6, no. 6, p. 066001, 2009.

[14]. Flint RD, Rosenow JM, Tate MC, and Slutzky MW, “Continuous decoding of human grasp kinematics using epidural and subdural signals,” J. Neural Eng, vol. 14, no. 1, p. 016005, 2017.

[15]. Flint RD et al., “Extracting kinetic information from human motor cortical signals,” NeuroImage, vol. 101, pp. 695–703, 11 2014. [PubMed: 25094020]

[16]. Delorme A. and Makeig S, “EEGLAB: an open source toolbox for analysis of single-trial EEG dynamics including independent component analysis,” J. Neurosci. Methods, vol. 134, no. 1, pp. 9–21, 3 2004. [PubMed: 15102499]

[17]. Goncharova II, McFarland DJ, Vaughan TM, and Wolpaw JR, “EMG contamination of EEG: spectral and topographical characteristics,” Clin. Neurophysiol, vol. 114, no. 9, pp. 1580–1593, 9 2003. [PubMed: 12948787]

[18]. Mehring C. et al., “Comparing information about arm movement direction in single channels of local and epicortical field potentials from monkey and human motor cortex,” J. Physiol.-Paris, vol. 98, no. 4, pp. 498–506, 7 2004. [PubMed: 16310349]

[19]. Flint RD, Lindberg EW, Jordan LR, Miller LE, and Slutzky MW, “Accurate decoding of reaching movements from field potentials in the absence of spikes,” J. Neural Eng, vol. 9, no. 4, p. 046006, 8 2012.

[20]. Hunter IW and Korenberg MJ, “The identification of nonlinear biological systems: Wiener and Hammerstein cascade models,” Biol. Cybern, vol. 55, no. 2–3, pp. 135–144, 1986. [PubMed: 3801534]

[21]. Westwick DT, Pohlmeyer EA, Solla SA, Miller LE, and Perreault EJ, “Identification of multiple-input systems with highly coupled inputs: Application to EMG prediction from multiple intracortical electrodes,” Neural Comput, vol. 18, no. 2, pp. 329–355, 2006. [PubMed: 16378517]

[22]. Fagg AH, Ojakangas GW, Miller LE, and Hatsopoulos NG, “Kinetic trajectory decoding using motor cortical ensembles,” IEEE Trans. Neural Syst. Rehabil. Eng, vol. 17, no. 5, pp. 487–496, 2009. [PubMed: 19666343]

[23]. Miller KJ, Zanos S, Fetz EE, den Nijs M, and Ojemann JG, “Decoupling the cortical power spectrum reveals real-time representation of individual finger movements in humans,” J. Neurosci. Off. J. Soc. Neurosci, vol. 29, no. 10, pp. 3132–3137, 3 2009.

[24]. Wang PT et al., “Characterization of electrocorticogram high-gamma signal in response to varying upper extremity movement velocity,” Brain Struct. Funct, vol. 222, no. 8, pp. 3705–3748, 11 2017. [PubMed: 28523425]

[25]. Ball T, Kern M, Mutschler I, Aertsen A, and Schulze-Bonhage A, “Signal quality of simultaneously recorded invasive and non-invasive EEG,” NeuroImage, vol. 46, no. 3, pp. 708–716, 7 2009. [PubMed: 19264143]

[26]. Ganguly K. et al., “Cortical Representation of Ipsilateral Arm Movements in Monkey and Man,” J. Neurosci, vol. 29, no. 41, pp. 12948–12956, 10 2009. [PubMed: 19828809]

[27]. Ball T. et al., “Movement related activity in the high gamma range of the human EEG,” NeuroImage, vol. 41, no. 2, pp. 302–310, 6 2008. [PubMed: 18424182]

[28]. Darvas F, Scherer R, Ojemann JG, Rao RP, Miller KJ, and Sorensen LB, “High gamma mapping using EEG,” NeuroImage, vol. 49, no. 1, pp. 930–938, 1 2010. [PubMed: 19715762]

[29]. Castermans T, Duvinage M, Cheron G, and Dutoit T, “About the cortical origin of the low-delta and high-gamma rhythms observed in EEG signals during treadmill walking,” Neurosci. Lett, vol. 561, pp. 166–170, 2 2014. [PubMed: 24412128]

[30]. Ajiboye AB, Simeral JD, Donoghue JP, Hochberg LR, and Kirsch RF, “Prediction of Imagined Single-Joint Movements in a Person With High-Level Tetraplegia,” IEEE Trans. Biomed. Eng, vol. 59, no. 10, pp. 2755–2765, 10 2012. [PubMed: 22851229]

[31]. Bacher D. et al., “Neural Point-and-Click Communication by a Person With Incomplete Locked-In Syndrome,” Neurorehabil. Neural Repair, vol. 29, no. 5, pp. 462–471, 6 2015. [PubMed: 25385765]

[32]. Collinger JL et al., “High-performance neuroprosthetic control by an individual with tetraplegia,” The Lancet, vol. 381, no. 9866, pp. 557–564, 2 2013.

[33]. Flesher SN et al., “Intracortical microstimulation of human somatosensory cortex,” Sci. Transl. Med, vol. 8, no. 361, pp. 361ra141–361ra141, 10 2016.

[34]. Hochberg LR et al., “Neuronal ensemble control of prosthetic devices by a human with tetraplegia,” Nature, vol. 442, no. 7099, pp. 164–171, 7 2006. [PubMed: 16838014]

[35]. Vansteensel MJ et al., “Fully Implanted Brain–Computer Interface in a Locked-In Patient with ALS,” N. Engl. J. Med, vol. 375, no. 21, pp. 2060–2066, 11 2016. [PubMed: 27959736]

[36]. Gharabaghi A. et al., “From assistance towards restoration with epidural brain-computer interfacing,” Restor. Neurol. Neurosci, vol. 32, no. 4, pp. 517–525, 1 2014. [PubMed: 25015699]

[37]. Hyder AA, Wunderlich CA, Puvanachandra P, Gururaj G, and Kobusingye OC, “The impact of traumatic brain injuries: A global perspective,” NeuroRehabilitation, vol. 22, no. 5, pp. 341–353, 12007. [PubMed: 18162698]

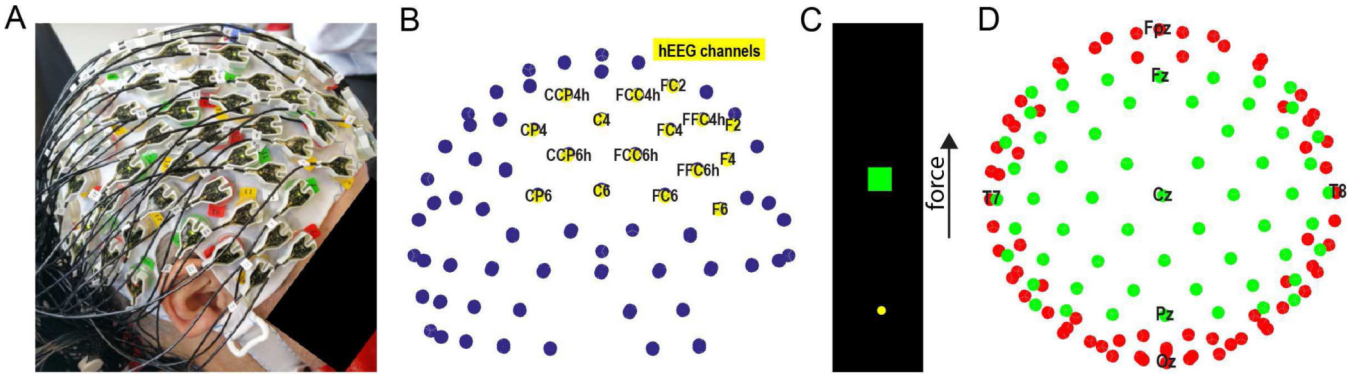

Fig. 1. Experimental setup.

(A) Subject wearing 128-electrode EEG actiCAP (B) Electrodes above hemicraniectomy (hEEG,yellow) shown for same subject from the same perspective. (C) Illustration of 1-dimensional continuous figure-flexion force matching task (D) Electrodes over the central (green) and peripheral (red) regions shown from overhead view

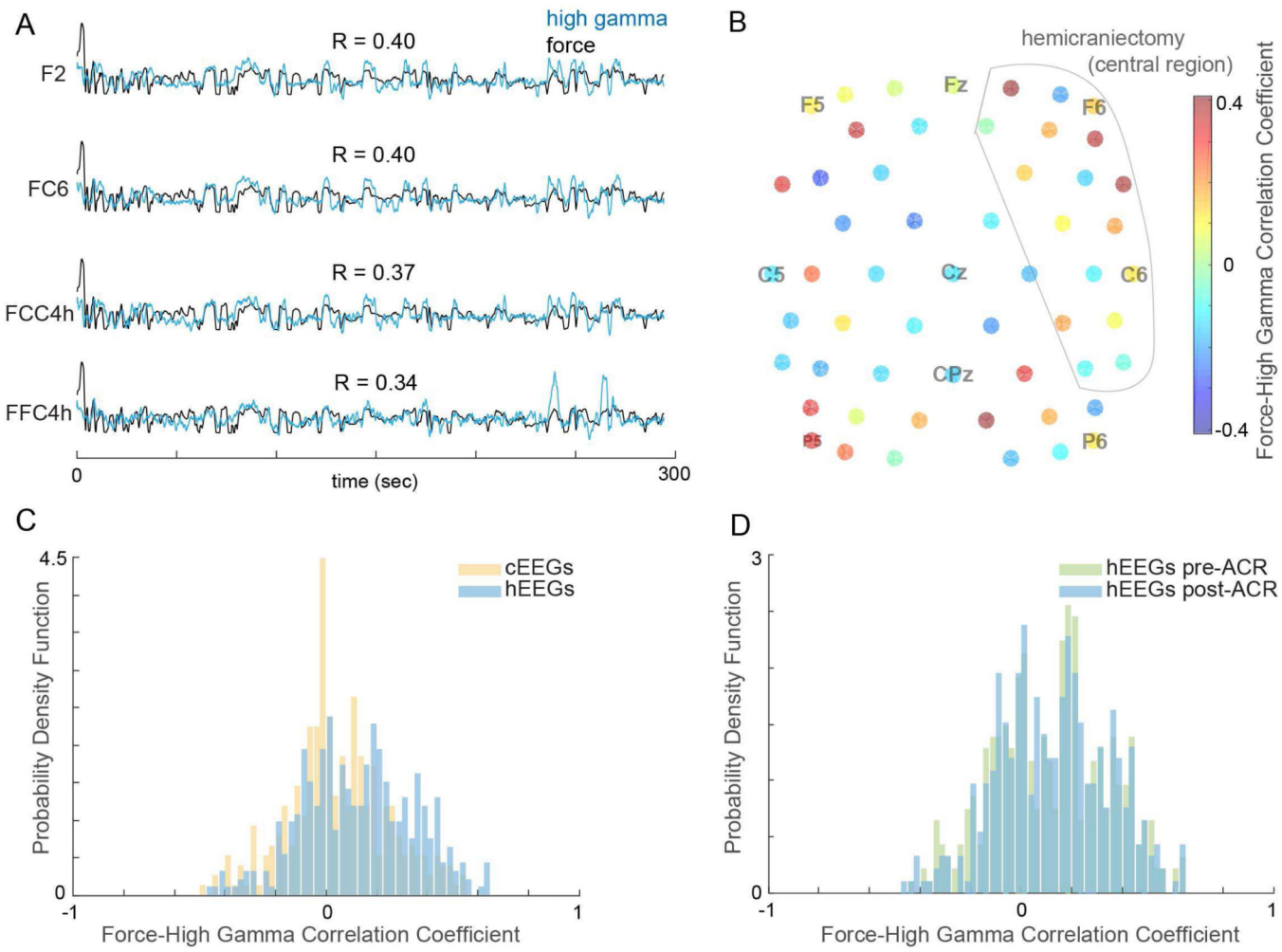

Fig. 2. Characteristics of hEEG.

(A) High gamma signal (blue) recorded from four hEEG electrodes overlaid on finger flexion force (black) in one run. (B) Correlations between HG and force from electrodes in the central region from same run. (C) Distributions of force-HG correlations for hEEG and cEEG after ACR. (D) Distributions of force-HG correlations for hEEG before and after ACR

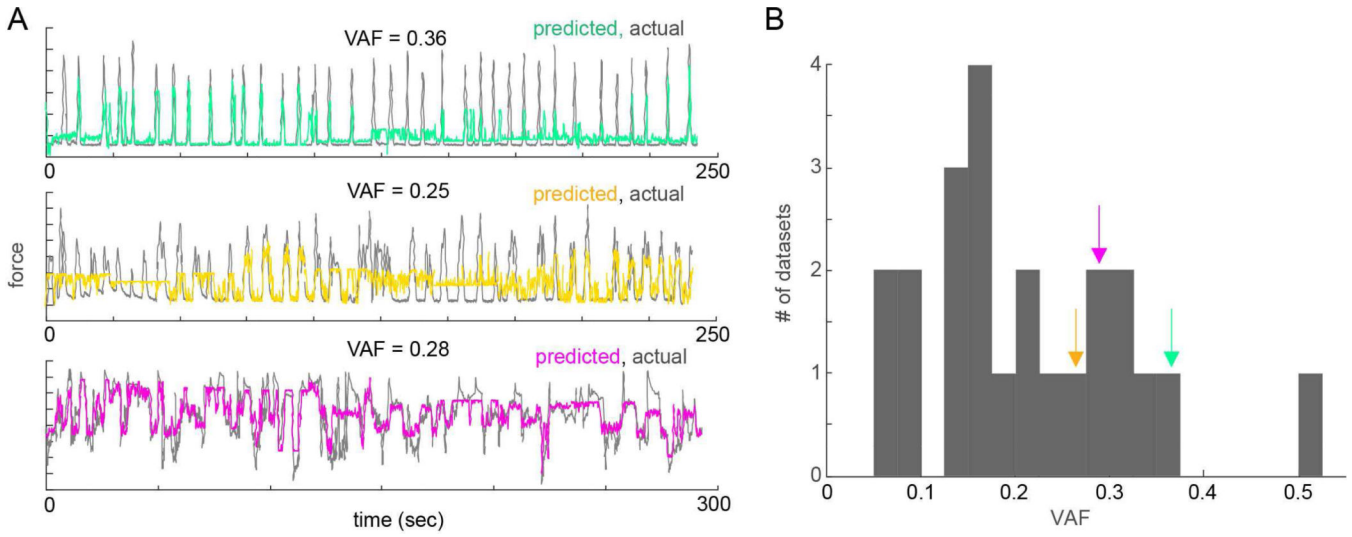

Fig. 3. Decoding flexion force from hEEG.

(A) Overlaid traces of predicted (color) vs actual (gray) finger flexion force in three datasets from three subjects. VAF for each run labeled above each trace. (B) Distribution of decoding performance (VAF) across all datasets from all subjects (arrows indicate where decoding examples from A fall within distribution).

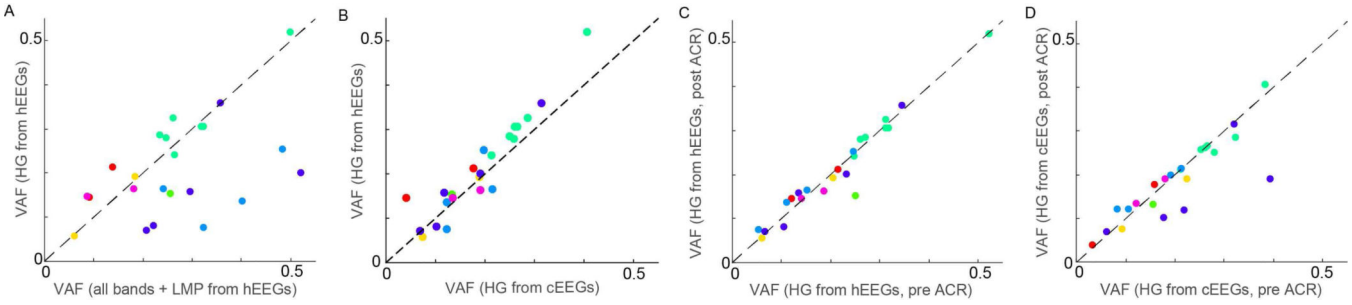

Fig. 4. Decoding performance comparisons.

(A) Decoding performance using only hEEG HG correlated with all-feature decoding performance over all subjects (dots denote runs, colored by subject). (B) Performance of decoders that use high gamma signals from hEEG vs. from cEEG. (C) Performance of decoders that use high gamma signals from hEEG pre- vs. post-ACR. (D) Performance of decoders that use high gamma signals from cEEG pre- vs. post-ACR.